IMMUNOHISTOCHEMICAL CHARACTERIZATION OF NEURONAL CILIA IN THE RAT CENTRAL NERVOUS SYSTEM

Rhome Hughes, B.A.

Thesis Prepared for the Degree of

MASTER OF SCIENCE

UNIVERSITY OF NORTH TEXAS

May 2002

APPROVED:

Harris Schwark, Major Professor
Jannon Fuchs, Major Professor
Guenter Gross, Minor Professor
Earl Zimmerman, Chair of the Department of Biological Sciences
C. Neal Tate, Dean of the Robert B. Toulouse School of Graduate Studies

Hughes, Rhome, Immunohistochemical characterization of neuronal cilia in the rat central nervous system. Master of Science (Biology), May 2002, 41 pp., 4 tables, 11 illustrations, references, 26 titles.

An anti-$G_{\alpha 11}$ antibody was used to label neuronal cilia throughout the rat central nervous system. Immunoreactive cilia were observed in every examined region of the rat CNS, but not in monkey or mouse tissue. Antibodies to $G_{\alpha q}$ and $G_{\alpha q/11}$ failed to label cilia. Immunoreactive cilia were observed as early as postnatal day 0 in spinal tissue, and postnatal day 3 in hypothalamic tissue. There was a statistically significant negative correlation between a region's mean cilium length and that region's distance to the nearest ventricle; regions nearest ventricles were those with the longest cilia. This correlation suggests neuronal cilia may function as chemosensors, detecting substances as they move out from the cerebrospinal fluid and into the extracellular space of the brain.

TABLE OF CONTENTS

LIST OF TABLES

LIST OF ILLUSTRATIONS

INTRODUCTION

Background Information

The presence of cilia have long been reported in the nervous system. Olfactory cilia have been well characterized as chemosensors, binding odorants to specific odorant receptors and initiating signal transduction. Bundles of motile cilia are also well recognized on ependymal cells that line the ventricles of the brain and the central canal of the spinal cord. The occurrence of neuronal cilia - solitary, non-motile cilia extending from neuronal somata and displaying a 9+0 microtubule pattern - have also been described, but these primary cilia have received considerably less attention despite their seemingly pervasive presence throughout the nervous system. Ultrastructural studies of the nervous system have localized these neuronal cilia in areas such as the inner nuclear and ganglion cell layers of the retina of guinea pigs and humans (Allen, 1965), in the lateral geniculate nucleus (Karlsson, 1966) and the lateral vestibular nucleus of the rat (Sotelo and Palay, 1968), in the preoptic nucleus of the rat (Peters et al., 1976), in the rat cerebral cortex (Dahl, 1963), in the fascia dentata of the rat hippocampal formation (Dahl, 1963), in the guinea pig hypothalamus (Vigh-Teichmann et al., 1980), and in the dorsal gray column of the rat spinal cord in or near the substantia gelatinosa (Duncan et al., 1963). Neuronal cilia have also been described in the dopaminergic tyrosine hydroxylase-immunoreactive neurons of the rat ventral tegmental area (Bayer and Pickel, 1990), and in the neuropeptide Y-immunoreactive neurons of the rat striatum (Wolfram

and Nitsch, 1992). Immunocytochemical studies have identified two receptors localized to the plasma membrane of neuronal cilia: the serotonin receptor 5-HT_6 (Brailov et al., 2000) and the somatostatin receptor sst_3 (Handel et al., 1999). 5-HT_6 receptor immunostaining was found in neuronal cilia in the rat striatum, nucleus accumbens, olfactory tubercle, and islands of Calleja (Brailov et al., 2000). Much more widespread were the sst_3 immunoreactive neuronal cilia, which were identified within areas of each of the following regions of the rat central nervous system: the main olfactory bulb, cerebral cortex, hippocampus, basal ganglia, septal and basal forebrain regions, amygdala and related areas, thalamus, hypothalamus, midbrain, pons, medulla oblongata, cerebellum, and spinal cord (Handel et al., 1999).

Where described, neuronal cilia arise as solitary projections from invaginations of the perikarya; the cilia display a 9+0 microtubule pattern in their basal bodies and proximal segments, while showing a 8+1 pattern in their more distal segments (Dahl, 1963; Duncan et al., 1963; Allen, 1965; Karlsson, 1966; Sotelo and Palay, 1968; Peters et al., 1976; Chalfie and Thomson, 1982; Bayer and Pickel, 1990; Brailov et al., 2000). Cilia of other body tissues, typically occurring in bundles, show a 9+2 microtubule pattern and these cilia are motile. In contrast, cilia with a 9+0 pattern, such as neuronal cilia, are presumably non-motile (Barnes, 1961; Peters et al., 1976; Handel et al., 1999). The basal body of a neuronal cilium represents the cell's distal centriole (Allen, 1965; Wheatley, 1995); in electron microscopy studies of primary cilia in other tissues, the basal body appears to have developed ontogenetically from a structure indistinguishable from a centriole (Barnes, 1961). The basal body extends to or protrudes slightly beyond

the soma's plasma membrane, and consists of nine evenly spaced triplets of microtubules arranged in cylindrical form, continuous with the filaments of the cilium (Allen, 1965; Peters et al., 1976). There is also usually a proximal centriole located near the basal body and oriented at nearly right angles with respect to it, which also displays the same 9+0 pattern of microtubule triplets (Dahl, 1963; Allen, 1965; Peters et al., 1976). From both the basal body and proximal centriole, thin rootlets resembling small ladders radiate into the surrounding cytoplasm, curving as they converge and ending in proximity to the Golgi apparatus (Dahl, 1963; Allen, 1965; Peters et al., 1976; Bayer and Pickel, 1990).

The proximal segment of the cilium contains a 9+0 pattern of longitudinal microtubule doublets, and as the doublets extend distally the arrangement of microtubules changes to a 8+1 pattern (Dahl, 1963; Duncan et al., 1963; Allen, 1965; Sotelo and Palay, 1968; Peters et al., 1976; Chalfie and Thomson, 1982; Bayer and Pickel, 1990; Brailov et al., 2000). This pattern results from the central displacement of one of the peripheral filaments, though the aberrant doublet does not come to occupy the true center of the arrangement, and the remaining eight doublets subsequently adjust their positions so as to remain evenly spaced (Duncan et al., 1963; Allen, 1965; Peters et al., 1976). This pattern remains until the most distal tip of the cilium (Allen, 1965). It has been offered that this change in filament pattern: (1) is regressive, and the cilium vestigial; (2) occurred to meet a new functional demand; (3) was an accident (Dahl, 1963). Based on the common occurrence of neuronal cilia and the consistency of their internal structure, the first and third of these explanations can be considered as unlikely,

and therefore in this regard it may be that these cilia have adapted to serve unique sensory functions (Allen, 1965).

Statement of Purpose

The aim of this project was to investigate a novel immunolocalization of neuronal cilia in the central nervous system of the rat using an anti-$G_{\alpha 11}$ antibody. The principal investigative goals included: (1) characterizing the immunoreactivity of the cilia through the use of additional antibodies and tissue from other species; (2) detailing the anatomical locations of $G_{\alpha 11}$-immunoreactive (IR) cilia throughout the central nervous system of the adult rat; (3) examining the developmental emergence of $G_{\alpha 11}$-IR cilia in prenatal / neonatal rat pups; and (4) scrutinizing those physical characteristics of either the cilia or the somata on which they appeared that could lend insight toward determining a possible physiological function.

Significance of the Problem

Since the first reports of their existence, there have been numerous postulates as to the function of neuronal cilia with little evidence to support any position. Perhaps the most prevailing line of thought, leading to the apparent neglect with which neuronal cilia have been treated, is that they are merely vestigial and functionless remnants (Peters et al., 1976). Others have suggested sensory functions, such as possible mechanoreceptors (Allen, 1965), or chemosensors (Barnes, 1961). With the discovery of 5-HT_6 and sst_3 receptors on the plasma membranes of neuronal cilia, it now seems more likely that they

could indeed be functional, serving as interfaces with the extracellular environment, similar to the function of olfactory cilia (Handel et al., 1999; Brailov et al., 2000). Neuronal cilia might provide a receptive surface capable of sensing specific molecules in the cell's immediate milieu, and the discovery of signal transduction machinery in neuronal cilia (as found in olfactory cilia) would lend increasing support to this hypothesis.

It has already been revealed that the motile cilia of ependymal cells lining the ventricular cavities contain a specific G protein subunit (G_{i2}), and this subunit could likely function as a transducer in the movement of these cilia (Shinohara et al., 1998). There are also distinct G protein subunits in olfactory cilia; a G_s-like protein mediates odor-induced cAMP production, whereas a G_o-like protein mediates odor-induced IP_3 formation (Schandar et al., 1998). In addition, a $G_{\alpha q}$ and $G_{\alpha 11}$ subunit have been shown to be present at the apical surface of cells within the olfactory tissue of the rat and catfish, where they most likely play a role in olfaction (Dellacorte et al., 1996). If similar subunits are also present within the membranes of neuronal cilia, it would not only be the first localization of a G protein subunit inside these cellular organelles, but would further aid in the assertion that neuronal cilia do possess a physiological function, plausibly of a nature concerning chemosensation.

MATERIALS AND METHODS

Subjects

The tissue sections studied came from subjects including: (1) adult male Long-Evans hooded and Sprague Dawley rats; (2) Long-Evans hooded rat pups collected on embryonic day 18 (E18), the day of birth (P0), and postnatal day 3 (P3); (3) adult male Balb-C/ICR mix mice; (4) adult $G_{\alpha 11}$ -/- mutant and $G_{\alpha q}$ -/- mutant mice (this tissue came from prior experiments in the laboratory) ; (5) an adult male bonnet macaque monkey (provided by E.G. Jones at the University of California at Davis); and (6) an adult male rhesus macaque monkey (provided by Chris Muly at Emory University).

Antibodies

The main primary antibody used was a rabbit polyclonal IgG antibody directed against an amino terminal domain of the $G_{\alpha 11}$ subunit, obtained from Santa Cruz Biotechnology (catalog #sc-394). An anti-$G_{\alpha q}$ antibody directed against an amino terminal domain of the $G_{\alpha q}$ subunit (catalog #sc-393), and a combined anti-$G_{\alpha q/11}$ antibody directed against a domain common to both subunits (catalog #sc-392) were also obtained, in addition to the blocking peptides for each antibody.

Tissue Preparation

Rats and mice were deeply anesthetized with either a urethane solution (1g/kg) or Nembutal solution (80 mg/kg) administered i.p., and then transcardially perfused with a 0.9% saline solution followed by a 4% paraformaldehyde solution in 0.1 M phosphate buffer (pH 7.4). The spinal cords and brains were rapidly removed, blocked, and then post-fixed in the same fixative solution for 1 h at 4˚C. The tissues were then cryoprotected in a 30% sucrose solution in 0.1 M phosphate buffer for approximately 48 h, and frozen in powdered dry ice and stored at -80˚C.

The bonnet macaque spinal cord tissue was perfused with a 4% paraformaldehyde solution in 0.1 M phosphate buffer and post-fixed overnight in 4% paraformaldehyde in phosphate buffer. The rhesus macaque brain tissue was perfused with a 4% paraformaldehyde, 0.2% gluteraldehyde, 15% picric acid solution, and post-fixed for 2-5 h in a 4% paraformaldehyde solution. The bonnet macaque spinal cord tissue was provided as frozen blocks, whereas the rhesus macaque brain tissue was sectioned at a thickness of 50μm and shipped in cryoprotectant solution.

Immunohistochemistry

Frozen tissue samples were sectioned at a thickness of 40 μm using a sliding microtome (with the exception of the rhesus macaque brain tissue, as previously noted). The sections were collected in Tris-buffered saline (TBS; pH 7.6), or if previously sectioned removed from cryoprotectant solution and rinsed in TBS. Sections were then submerged in a pre-incubation solution comprised of TBS with 5% normal goat serum

(NGS) and 0.1% Triton X-100 for 30 min at room temperature (RT). All incubations were performed under continuous gentle agitation. Tissue sections were then incubated with the primary antibody of choice at an optimal dilution of 1:3,000 for spinal cord tissue, and 1:1,500 for brain tissue, in pre-incubation solution at 4°C overnight. For adsorption control, the blocking peptide for the antibody of use was added to this solution.

Upon completion of incubation in the primary antibody solution, tissue sections were washed in a 15 min rinse of TBS, a 15 min rinse of pre-incubation solution, and then incubated with a secondary antibody (goat anti-mouse; Jackson ImmunoResearch Laboratories) at an optimal dilution of 1:1,000 for either spinal cord or brain tissue, for 1 h in pre-incubation solution at RT. After two 15 min rinses in TBS with 1% NGS, the tissue sections were processed with an ABC solution (50 µl each of Vector Standard A and B solutions in 2.5 ml of TBS with 1% NGS and 0.0365 g NaCl), providing biotin amplification. Tissue sections were then washed in two 15 min rinses of TBS before incubation in a TBS solution containing (per 5 ml of TBS) 2.5 mg 3,3'-diaminobenzidine and 2 µl of 50% hydrogen peroxide. Tissue sections were allowed to react in this solution for 2 min, and then were washed in two 15 min rinses of TBS. Tissue sections then were mounted onto subbed slides, dehydrated through a series of ethanol solutions (50%, 70%, 95%, 100% and 100%), cleared in three consecutive xylene solutions, and then coverslipped with DPX mounting medium. When desired, the tissue sections were counterstained with thionin and differentiated in an acidified 95% ethanol solution.

Serial Sections through the Adult Rat Brain

In order to obtain a series of sections throughout the whole adult rat brain, coronal sections were taken through an entire brain and stored in a 30% glycerol and 30% ethylene glycol in 0.1 M phosphate buffer cryoprotectant solution at -20°C for no longer than three months. Every tenth section was then processed for immunohistochemistry. This equated to a 0.4 mm distance between sections and ensured that most of the principal regions, layers, and nuclei of the brain would be present.

Data Analysis

Sections that were immunohistochemically processed, Nissl counterstained, and mounted were examined for the presence of immunoreactive cilia via light microscopy. Specific regions of the CNS were chosen to represent the range of neuronal cilia length and somata sizes. Within these selected regions, approximately 30 to 50 cilia and 30 to 50 somata outlines were drawn separately with the aid of a camera lucida. Those cilia selected for drawing were those who lay horizontal across the plane of the section, and thus their entire length could be brought into focus at the same level; those somata selected for drawing were those who appeared to be sectioned through their center, as evident by a detectable nucleus, and were thus at or near their maximum width. The drawings were then digitized and analyzed using image-analysis software (AIS 6.0 Rev. 1.0, Imaging Research Inc.). Portions of the data presented have been previously published in abstracts (Fuchs et al., 2000; Schwark and Fuchs, 2000).

RESULTS

Immunostaining of Neuronal Cilia

Tissue sections from the spinal cords and brains of rats, mice, and monkeys were analyzed for the presence of immunoreactive neuronal cilia. Results from experiments using the anti-$G_{\alpha q}$ antibody, the anti-$G_{\alpha q/11}$ antibody, and all those using the mutant mice tissue were generated in the laboratory prior to this study. Of the three antibodies used, only the anti-$G_{\alpha 11}$ antibody provided staining of neuronal (or ependymal) cilia. Furthermore, $G_{\alpha 11}$-IR cilia were identified only in rat tissue, and only at or after postnatal day 0. The results from these experiments are presented in Table 1.

Table 1. Immunostaining of neuronal cilia

Antibody	Species	Subject	Tissue	IR neuronal cilia	IR ependymal cilia
anti-$G_{\alpha 11}$	rat	E18	spinal cord	-	-
			brain	-	-
		PO	spinal cord	+	+
			brain	-	+
		P3	spinal cord	+	+
			brain	+	+
		adult	spinal cord	+	+
			brain	+	+
	mouse	adult	spinal cord	-	-
			brain	-	-
		$G_{\alpha 11}$-/-*+	spinal cord	-	-
		$G_{\alpha q}$-/-*+	spinal cord	-	-
	monkey	adult	spinal cord	-	-
			brain	-	-
anti-$G_{\alpha q/11}$+	rat	adult	spinal cord	-	-
			brain	-	-
	mouse	adult	spinal cord	-	-
			brain	-	-
		$G_{\alpha 11}$-/-*	spinal cord	-	-
		$G_{\alpha q}$-/-*	spinal cord	-	-
anti-$G_{\alpha q}$+	rat	adult	spinal cord	-	-
	mouse	adult	spinal cord	-	-

*Tissue came from prior experiments in the laboratory
+Results generated in prior experiments in the laboratory

Immunolocalization of Neuronal Cilia in the Adult Rat CNS

A nearly ubiquitous presence of $G_{\alpha 11}$-IR neuronal cilia was revealed within the adult rat CNS upon analysis of a series of tissue sections containing most of the principal regions, layers, and nuclei of the CNS (Table 2). Cilia were always observed as a single cilium per soma, and were never observed on glial cells.

In addition to determining whether $G_{\alpha 11}$-IR cilia were present or absent, each region was evaluated in terms of its percentage of ciliated neurons, or the percentage of somata in an region that were expressing $G_{\alpha 11}$-IR cilia. Regions recorded as having a high percentage of ciliated neurons were those in which all, or nearly all, somata were found to possess a cilium; because somata were viewed from a fixed perspective, and the possibility existed that a soma may have been divided during sectioning, it could not be determined that a soma found to be lacking a cilium did not indeed possess a cilium outside that limited range of view. Regions recorded as having a low percentage of ciliated neurons were those in which the percentage of somata not expressing cilia was great enough to most likely require additional explanations beyond those associated with sectioning, as mentioned above. These regions with a low percentage of ciliated neurons were much less common than those with a high percentage of ciliated neurons, and included certain layers of the olfactory bulb, the septal nuclei, the medial geniculate nucleus, and the cerebellar cortex.

Table 2. Immunolocalization of neuronal cilia in the adult rat CNS

	Presence of $G_{\alpha 11}$-IR cilia	Percentage of ciliated neurons
Telencephalon		
Olfactory system		
Olfactory bulb: glomerular layer	+	low
external plexiform layer	+	low
mitral cell layer	+	high
internal plexiform layer	+	low
internal granular layer	+	high
ependymal layer	+	low
Accessory olfactory bulb	+	high
Anterior olfactory nucleus	+	high
Olfactory tubercle	+	high
Islands of Calleja	+	high
Nucleus of the lateral olfactory tract	+	high
Bed nucleus, accessory olfactory tract	+	high
Cerebral cortex		
Frontal	+	high
Parietal	+	high
Temporal	+	high
Cingulate	+	high
Retrospenial	+	high
Piriform	+	high
Perirhinal	+	high
Occipital	+	high
Entorhinal	+	high
Insular	+	high
Tenia tecta	+	high
Indusium griseum	+	high
Hippocampal formation and associated areas		
CA1	+	high
CA2	+	high
CA3	+	high
Dentate gyrus	+	high
Presubiculum	+	high
Parasubiculum	+	high
Subiculum	+	high

	Presence of $G_{\alpha 11}$-IR cilia	Percentage of ciliated neurons
Basal Ganglia		
Caudate putamen	+	high
Nucleus accumbens	+	high
Globus pallidus	+	high
Claustrum	+	high
Ventral pallidum	+	high
Subthalamic nucleus	+	high
Amygdala areas		
Basolateral nuclear group	+	high
Corticomedial nuclear group	+	high
Central amygdaloid nucleus	+	high
Septal areas		
Medial septal nucleus	+	low
Lateral septal nucleus	+	low
Diencephalon		
Thalamus		
Anterior nuclear group	+	high
Midline nuclear group	+	high
Mediodorsal nucleus	+	high
Intralaminar nuclear group	+	high
Lateral nuclear group	+	high
Ventral nuclear group	+	high
Lateral geniculate nucleus	+	high
Medial geniculate nucleus	+	low
Posterior nuclear group	+	high
Hypothalamus		
Preoptic nuclear group	+	high
Suprachiasmatic nuclear group	+	high
Tuberal nuclear group	+	high
Mammillary nuclear group	+	high
Mesencephalon		
Pretectal region	+	high
Superior colliculus	+	high
Inferior colliculus	+	high
Oculomotor nuclear group	+	high
Midbrain reticular formation	+	high

	Presence of $G_{\alpha 11}$-IR cilia	Percentage of ciliated neurons
Red nucleus	+	high
Periaqueductal grey matter	+	high
Interpeduncular nucleus	+	high
Ventral tegmental area	+	high
Substantia nigra	+	high
Metencephalon		
Pons		
Trigeminal nuclei	+	high
Pontine reticular formation	+	high
Superior olivary complex	+	high
Locus coeruleus	+	high
Cerebellum		
Molecular layer of cortex	+	low
Purkinje cell layer of cortex	+	low
Granule cell layer of cortex	+	low
Cerebellar nuclei	+	high
Myelencephalon		
Medulla oblongata		
Vestibular nuclei	+	high
Cochlear nuclei	+	high
Medullary reticular formation	+	high
Solitary nucleus	+	high
Inferior olivary complex	+	high
Spinal Cord		
Dorsal horn	+	high
Ventral horn	+	high

Development of $G_{\alpha 11}$-IR Neuronal Cilia

Within the spinal cord, $G_{\alpha 11}$-IR neuronal cilia were absent at E18, but were present at P0, at which time they appeared on only a few neurons. Within three days (P3), their presence had dramatically increased such that they appeared on a percentage of somata comparable to that in adult tissue. $G_{\alpha 11}$-IR ependymal cilia were also absent at E18 and present at P0, though at P0 the percentage of ependymal cells expressing $G_{\alpha 11}$-IR ependymal cilia was closer to that of adult levels than was the percentage of neurons expressing $G_{\alpha 11}$-IR neuronal cilia. By P3, the percentage of ependymal cells expressing $G_{\alpha 11}$-IR cilia was also comparable to that in adult tissue.

Within hypothalamic tissue (selected for examination a priori for its abundant and easily visualized $G_{\alpha 11}$-IR neuronal cilia in adult sections), $G_{\alpha 11}$-IR neuronal cilia were absent in both E18 and P0 tissue. $G_{\alpha 11}$-IR neuronal cilia were present in P3 tissue, but occurred on fewer somata than in adult tissue. $G_{\alpha 11}$-IR ependymal cilia, however, were absent at E18 but present at P0. As in the spinal cord, by P3 the percentage of ependymal cells expressing $G_{\alpha 11}$-IR cilia was comparable to that in adult tissue (Table 3).

Table 3. Development of $G_{\alpha 11}$-IR neuronal cilia

a. Immunolocalization of cilia

	E18	P0	P3	Adult
Spinal Cord:				
neurons	-	+	+	+
ependymal cells	-	+	+	+
Hypothalamus:				
neurons	-	-	+	+
ependymal cells	-	+	+	+

b. Percentage of cells expressing $G_{\alpha 11}$-IR cilia

Spinal Cord:	
neurons	P0 << P3 = adult
ependymal cells	PO < P3 = adult
Hypothalamus:	
neurons	P3 < adult
ependymal cells	P0 < P3 = adult

Measurements of Cilia Lengths and Somata Areas in the Adult Rat CNS

Measurements of cilia lengths (ranging from mean values of 2.1 μm to 9.4 μm) and somata areas (ranging from mean values of 44.9 μm^2 to 1016.6 μm^2) were taken from selected regions of the adult rat CNS (Table 4). Regression analysis of the means revealed no statistically significant correlation between these two variables across CNS regions (Figure 1; $r = 0.048$, $df = 21$, $p > 0.05$). The distance from each region of the CNS to the nearest cerebrospinal fluid (CSF)-containing cavity was also recorded, and was measured as the distance from the center of the region to the nearest border of the nearest ventricle (or other CSF-containing cavity) using a stereotaxic atlas of the rat brain (Paxinos, 1986). Regression analysis revealed a statistically significant negative correlation between these two variables (Figure 2; $r = -0.613$, $df = 21$, $p < 0.01$), such that those regions closest to a ventricle displayed the longest cilia. Furthermore, those regions within an approximate 2 mm distance to the nearest ventricle retained this statistically significant negative correlation ($r = -0.608$, $df = 12$, $p < 0.05$), while those beyond this distance did not ($r = 0.415$, $df = 7$, $p > 0.05$). Each region's ratio of cilium length:soma area was also compared to that region's distance to the nearest ventricle. There was a statistically significant negative correlation between these two variables (Figure 3; $r = -0.482$, $df = 21$, $p < 0.05$), such that those regions closest to ventricles were those with the largest ratio of cilium length:soma area. Measurements of cilia lengths and somata areas taken from CNS regions with obvious similarities were further analyzed individually, and included those measurements from (1) different layers of the same cortical region, in which there was not a statistically significant correlation

between cilium length and soma area ($r = 0.732$, $df = 2$, $p > 0.05$), (2) regions defined as having a low percentage of ciliated neurons, and (3) different laminae of the same spinal region (Figures 4 - 6).

Table 4. Cilia lengths and somata areas in the adult rat CNS

CNS Region	Cilium length (μm)	S.D.	S.E.	n	Soma area (μm^2)	S.D.	S.E.	n	Cilium length: soma area (μm^{-1})
TELENCEPHALON									
Olfactory system									
Anterior olfactory nucleus									
medial part	**3.2**	0.6	0.1	50	**80.4**	24.2	4.1	36	**0.040**
Cerebral cortex									
Entorhinal									
layers 2/3	**3.5**	0.6	0.1	43	**116.5**	21.8	3.3	45	**0.030**
Frontal									
layers 2/3	**2.8**	0.4	0.1	40	**95.0**	18.8	3.0	41	**0.029**
layer 4	**2.3**	0.4	0.1	52	**65.5**	11.4	1.7	46	**0.035**
layer 5	**3.1**	0.4	0.1	48	**155.4**	76.5	11.9	42	**0.020**
layer 6	**3.1**	0.4	0.1	55	**86.6**	13.3	1.7	61	**0.035**
Occipital									
layers 2/3	**3.1**	0.4	0.1	53	**98.9**	18.1	2.6	49	**0.031**
Perirhinal									
layers 2/3	**3.2**	0.5	0.1	46	**108.3**	17.3	3.0	35	**0.029**
Hippocampus									
Dentate gyrus									
granular layer	**3.8**	0.5	0.1	71	**70.4**	16.2	2.5	43	**0.054**
Subiculum	**4.8**	0.6	0.1	47	**176.1**	27.6	4.2	45	**0.027**
Basal ganglia									
Caudate putamen	**4.9**	0.7	0.1	44	**94.7**	29.5	4.8	39	**0.052**
Septal areas									
Lateral septal nucleus	**5.1**	0.7	0.1	38	**86.1**	16.9	2.8	37	**0.059**

CNS Region	Cilium length (μm)	S.D.	S.E.	n	Soma area (μm^2)	S.D.	S.E.	n	Cilium length: soma area (μm^{-1})
DIENCEPHALON									
Thalamus									
Anterior nuclear group									
anterodorsal nucleus	**5.7**	1.2	0.2	38	**158.5**	32.2	5.0	43	**0.036**
Medial geniculate nucleus	**2.1**	0.3	0.1	22	**131.0**	17.0	3.0	34	**0.016**
Ventral nuclear group									
ventral posterior nucleus	**2.1**	0.4	0.1	46	**158.0**	30.6	5.2	36	**0.013**
Hypothalamus									
Preoptic nuclear group									
periventricular nucleus	**7.5**	1.2	0.2	44	**92.9**	18.9	3.0	41	**0.080**
Tuberal nuclear group									
arcuate nucleus	**6.0**	1.1	0.2	50	**105.5**	26.3	4.1	43	**0.057**
MESENCEPHALON									
Periaqueductal grey matter	**9.4**	1.4	0.2	34	**126.0**	39.6	6.9	34	**0.074**
METENCEPHALON									
Cerebellum									
Cerebellar nuclei	**4.1**	0.6	0.1	37	**294.2**	81.2	14.6	32	**0.014**
Molecular layer of cortex	**2.8**	0.4	0.1	41	**44.9**	9.7	1.7	34	**0.062**
MYELENCEPHALON									
Spinal Cord									
Lumbar region									
dorsal horn (l. 1-4)	**4.3**	0.9	0.1	43	**58.6**	12.3	2.2	32	**0.073**
ventral horn (l. 9)	**4.4**	0.9	0.2	22	**1016.6**	349.9	93.5	15	**0.004**
central canal (l. 10)	**5.7**	1.2	0.2	37	**153.8**	42.9	8.1	29	**0.037**

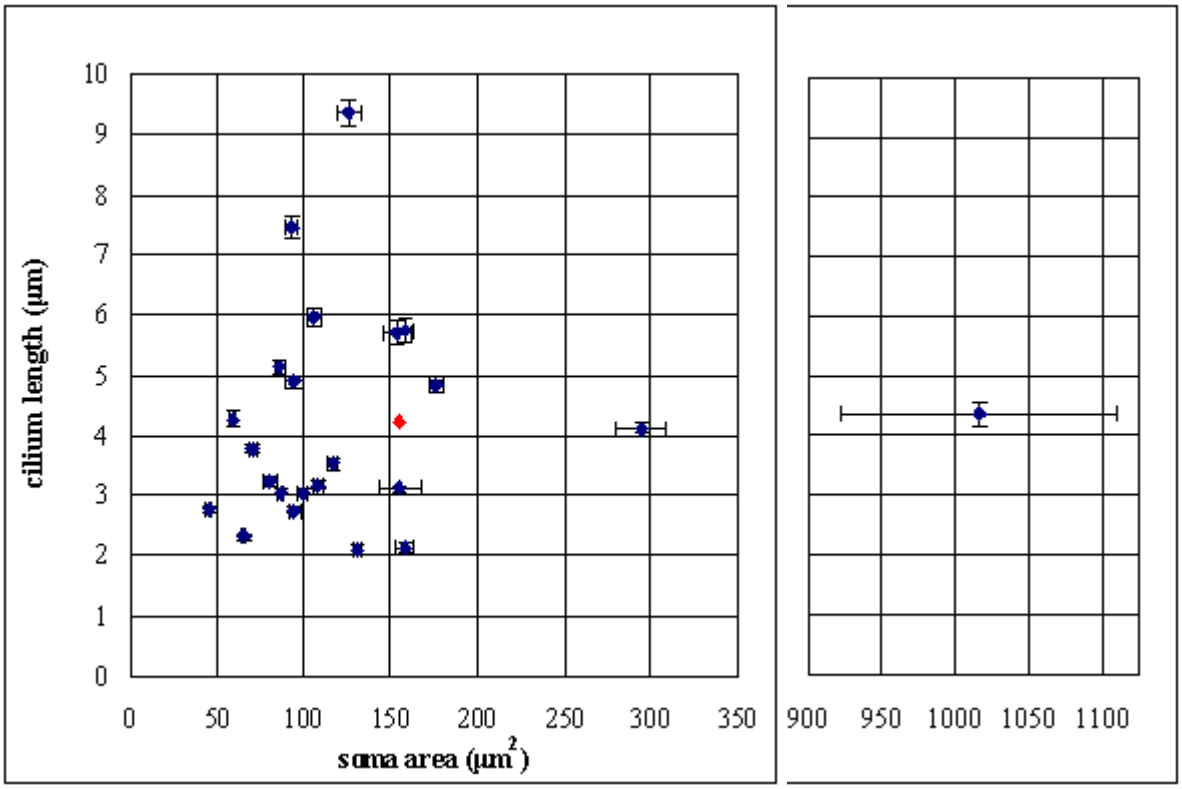

Figure 1. Cilium length versus soma area (mean ± sem; r = 0.048, df = 21, p > 0.05).

	Cilium length (µm)	Soma area (µm^2)
Medial geniculate nucleus	2.1	131.0
Ventral posterior nucleus - thalamus	2.1	158.0
Frontal cortex, layer 4	2.3	65.5
Frontal cortex, layers 2/3	2.8	95.0
Molecular layer of cerebellar cortex	2.8	44.9
Frontal cortex, layer 6	3.1	86.6
Occipital cortex, layers 2/3	3.1	98.9
Frontal cortex, layer 5	3.1	155.4
Perirhinal cortex, layers 2/3	3.2	108.3
Anterior olfactory nucleus, medial part	3.2	80.4
Entorhinal cortex, layers 2/3	3.5	116.5
Dentate gyrus, granular layer	3.8	70.4
Cerebellar nuclei	4.1	294.2
Dorsal horn (l. 1-4) of lumbar spinal cord	4.3	58.6
Ventral horn (l. 9) of lumbar spinal cord	4.4	1016.6
Subiculum	4.8	176.1
Caudate putamen	4.9	94.7
Lateral septal nucleus	5.1	86.1
Lamina 10 of lumbar spinal cord	5.7	153.8
Anterodorsal nucleus - thalamus	5.7	158.5
Arcuate nucleus - hypothalamus	6.0	105.5
Periventricular nucleus - hypothalamus	7.5	92.9
Periaqueductal grey matter	9.4	126.0
average	4.2	155.4

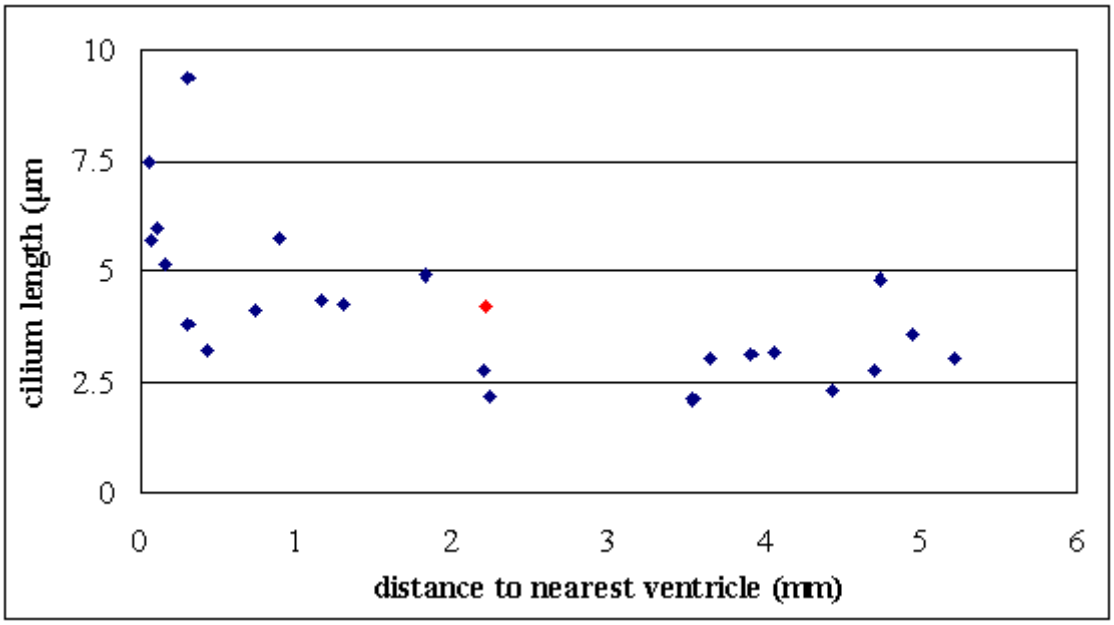

Figure 2. Cilium length versus distance to nearest ventricle ($r = -0.613$, $df = 21$, $p < 0.01$).

	Cilium length (µm)	Ventricular proximity (mm)
Medial geniculate nucleus	2.1	3.5
Ventral posterior nucleus - thalamus	2.1	2.2
Frontal cortex, layer 4	2.3	4.4
Frontal cortex, layers 2/3	2.8	4.7
Molecular layer of the cerebellar cortex	2.8	2.2
Frontal cortex, layer 6	3.1	3.7
Occipital cortex, layers 2/3	3.1	5.2
Frontal cortex, layer 5	3.1	3.9
Perirhinal cortex, layers 2/3	3.2	4.1
Anterior olfactory nucleus, medial part	3.2	0.4
Entorhinal cortex, layers 2/3	3.5	5.0
Dentate gyrus, granular layer	3.8	0.3
Cerebellar nuclei	4.1	0.7
Dorsal horn (l. 1-4) of lumbar spinal cord	4.3	1.3
Ventral horn (l. 9) of lumbar spinal cord	4.4	1.2
Subiculum	4.8	4.7
Caudate putamen	4.9	1.8
Lateral septal nucleus	5.1	0.2
Lamina 10 of lumbar spinal cord	5.7	0.1
Anterodorsal nucleus - thalamus	5.7	0.9
Arcuate nucleus - hypothalamus	6.0	0.1
Periventricular nucleus - hypothalamus	7.5	0.1
Periaqueductal grey matter	9.4	0.3
average	4.2	2.2

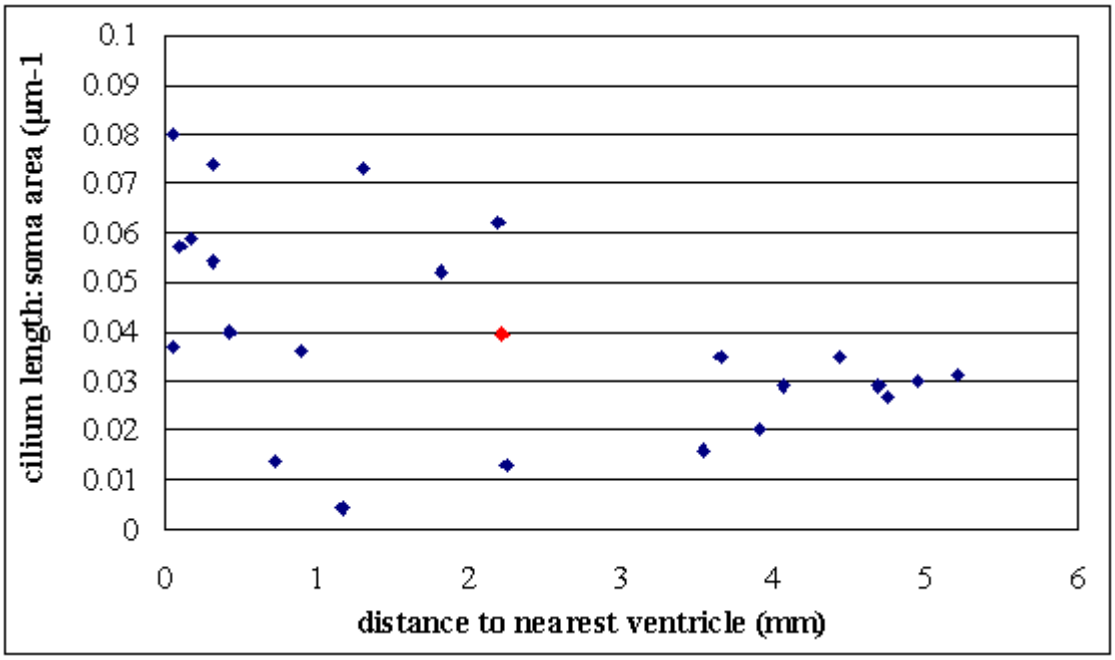

Figure 3. Cilium length:soma area versus distance to nearest ventricle (r = -0.482, df = 21, p <0.05).

	Cilium length:soma area (μm^{-1})	Ventricular proximity (mm)
Periventricular nucleus - hypothalamus	0.080	0.1
Lamina 10 of lumbar spinal cord	0.037	0.1
Arcuate nucleus - hypothalamus	0.057	0.1
Lateral septal nucleus	0.059	0.2
Dentate gyrus, granular layer	0.054	0.3
Periaqueductal grey matter	0.074	0.3
Anterior olfactory nucleus, medial part	0.040	0.4
Cerebellar nuclei	0.014	0.7
Anterodorsal nucleus - thalamus	0.036	0.9
Ventral horn (l. 9) of lumbar spinal cord	0.004	1.2
Dorsal horn (l. 1-4) of lumbar spinal cord	0.073	1.3
Caudate putamen	0.052	1.8
Molecular layer of the cerebellar cortex	0.062	2.2
Ventral posterior nucleus - thalamus	0.013	2.2
Medial geniculate nucleus	0.016	3.5
Frontal cortex, layer 6	0.035	3.7
Frontal cortex, layer 5	0.020	3.9
Perirhinal cortex, layers 2,3	0.029	4.1
Frontal cortex, layer 4	0.035	4.4
Frontal cortex, layers 2,3	0.029	4.7
Subiculum	0.027	4.7
Entorhinal cortex, layers 2,3	0.030	5.0
Occipital cortex, layers 2,3	0.031	5.2
average	0.039	2.2

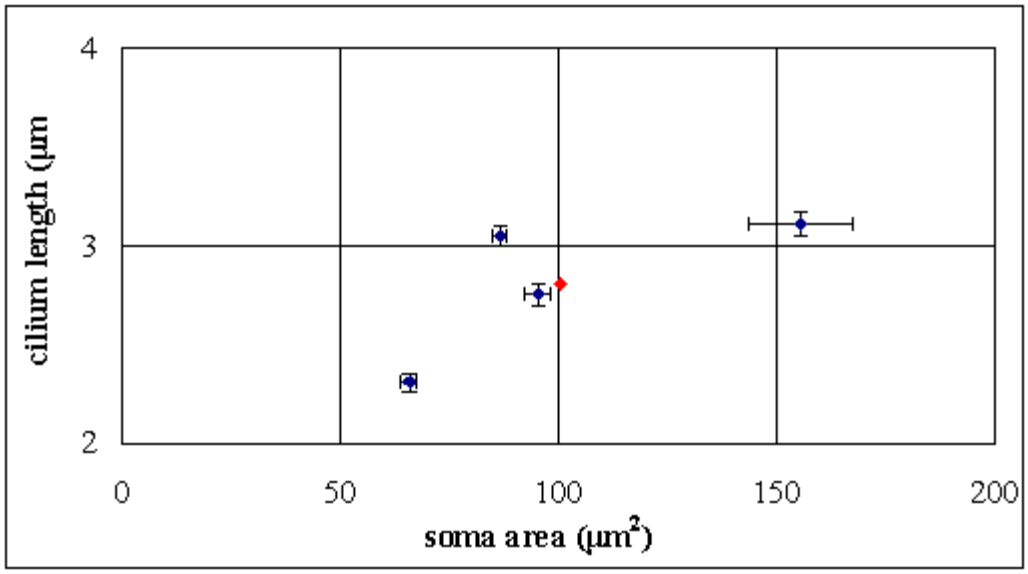

Figure 4. Cilium length versus soma area by layer in the frontal cortex (mean ± sem; r = 0.732, df = 2, p > 0.05).

	Soma area (µm²)	Cilium length (µm)
Layer 4	65.5	2.3
Layer 6	86.6	3.1
Layers 2/3	95.0	2.8
Layer 5	155.4	3.1
average	100.6	2.8

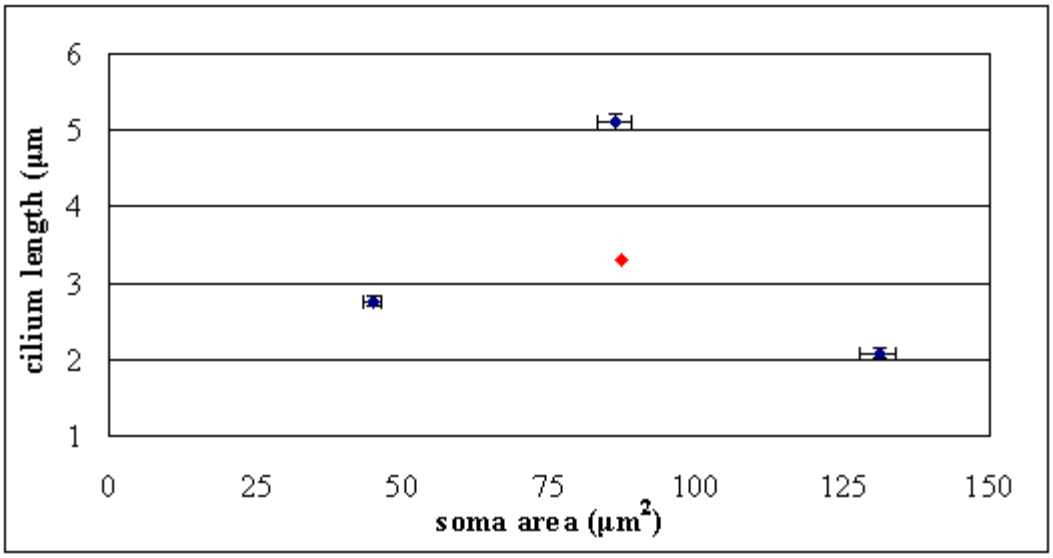

Figure 5. Cilium length versus soma area in regions with a low percentage of ciliated neurons (mean ± sem).

	Soma area (µm^2)	Cilium length (µm)
Molecular layer of cerebellar cortex	44.9	2.8
Lateral septal nucleus	86.1	5.1
Medial geniculate nucleus	131.0	2.1
average	87.4	3.3

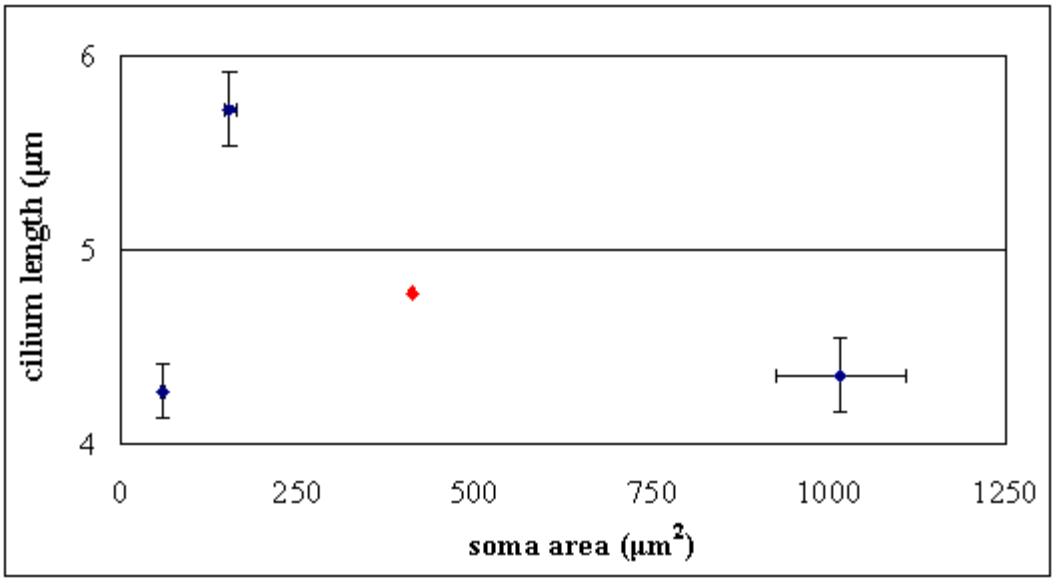

Figure 6. Cilium length versus soma area in the lumbar spinal cord (mean ± sem).

	Soma area (μm^2)	Cilium length (µm)
dorsal horn (laminae 1-4)	58.6	4.3
lamina 10	153.8	5.7
ventral horn (lamina 9)	1016.6	4.4
average	409.7	4.8

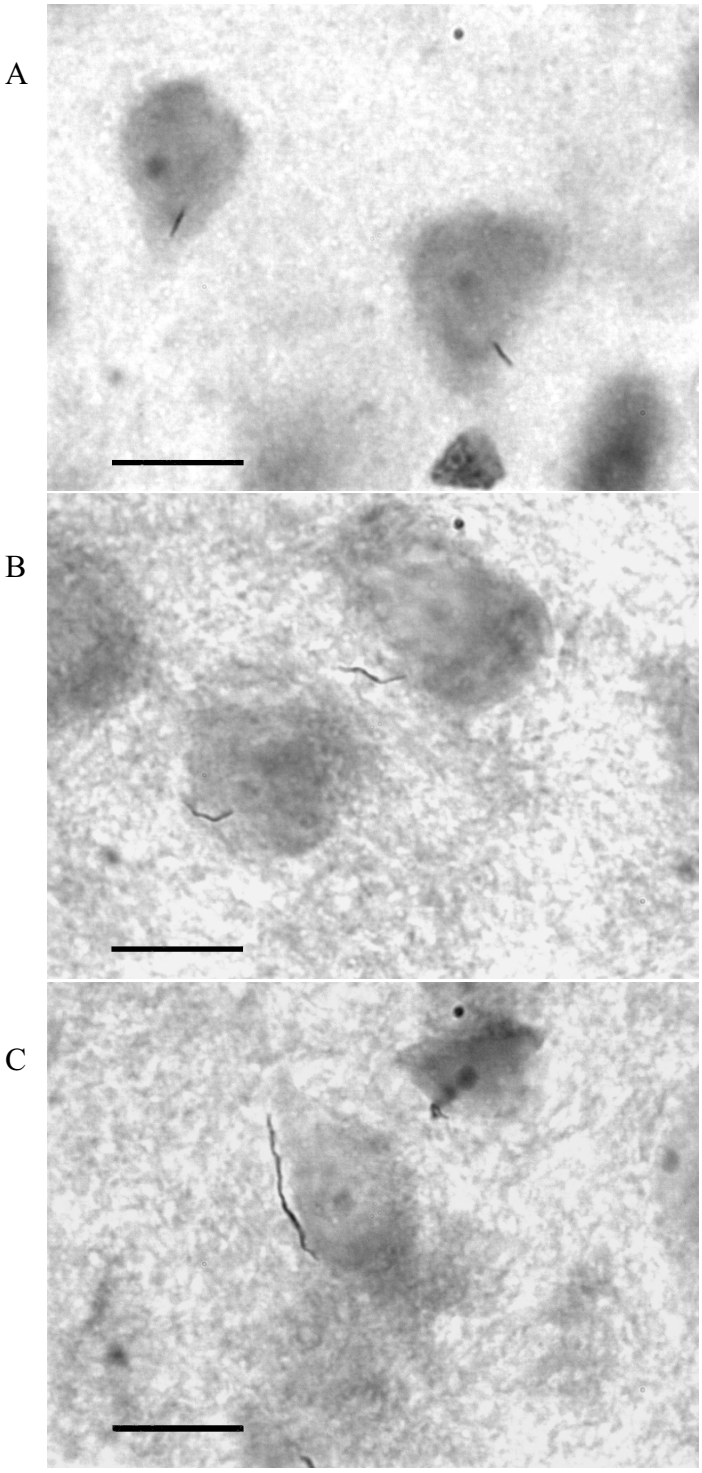

Figure 7. Comparison of lengths of neuronal cilia. Perikarya counterstained with thionin. *A*, Frontal cortex, layers 2/3 (mean length = 2.8 μm). *B*, Anterodorsal thalamic nucleus (mean length = 5.7 μm). *C,* Periaqueductal grey matter (mean length = 9.4 μm). Scale bar = 10 μm.

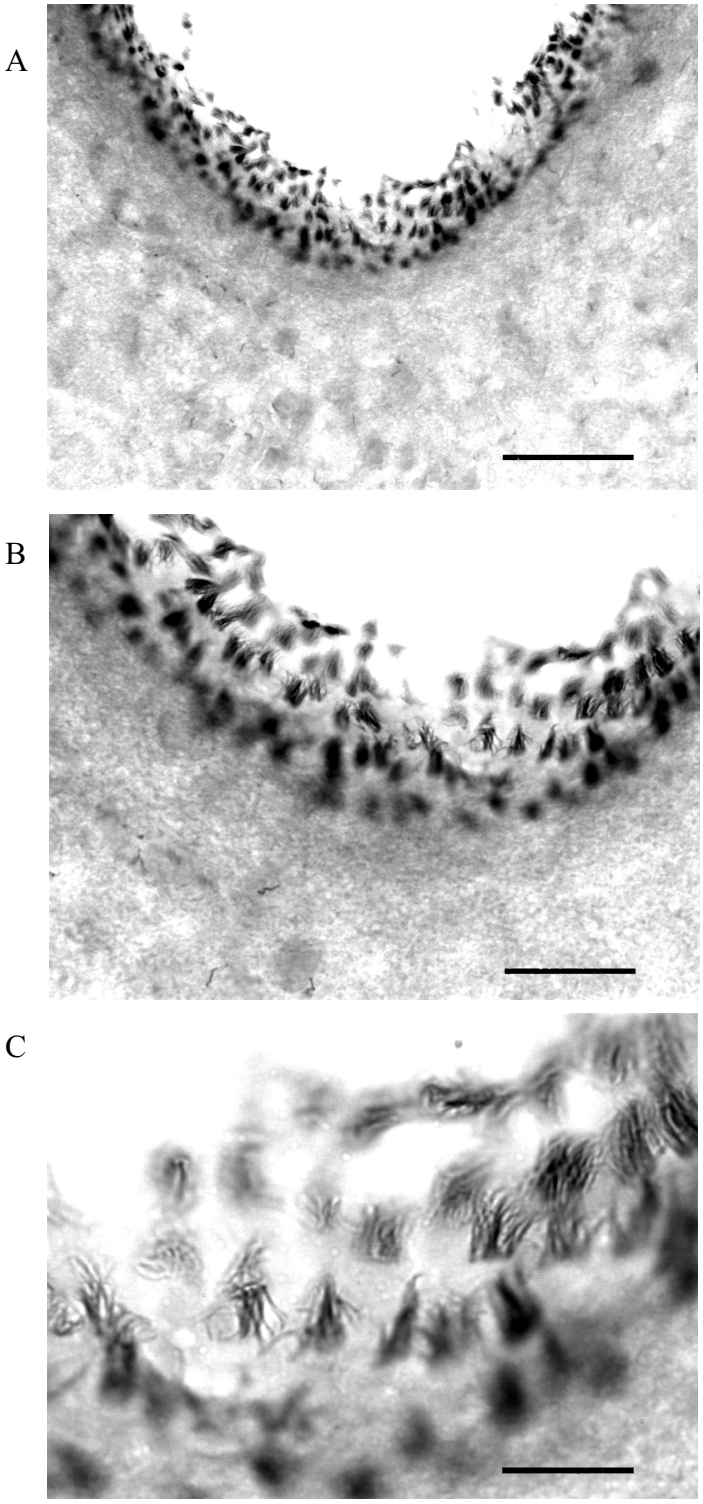

Figure 8. Ependymal cilia surrounding the third ventricle. Perikarya counterstained with thionin. Scale bar: in *A*, 50 μm; in *B*, 25 μm; in *C*, 10 μm.

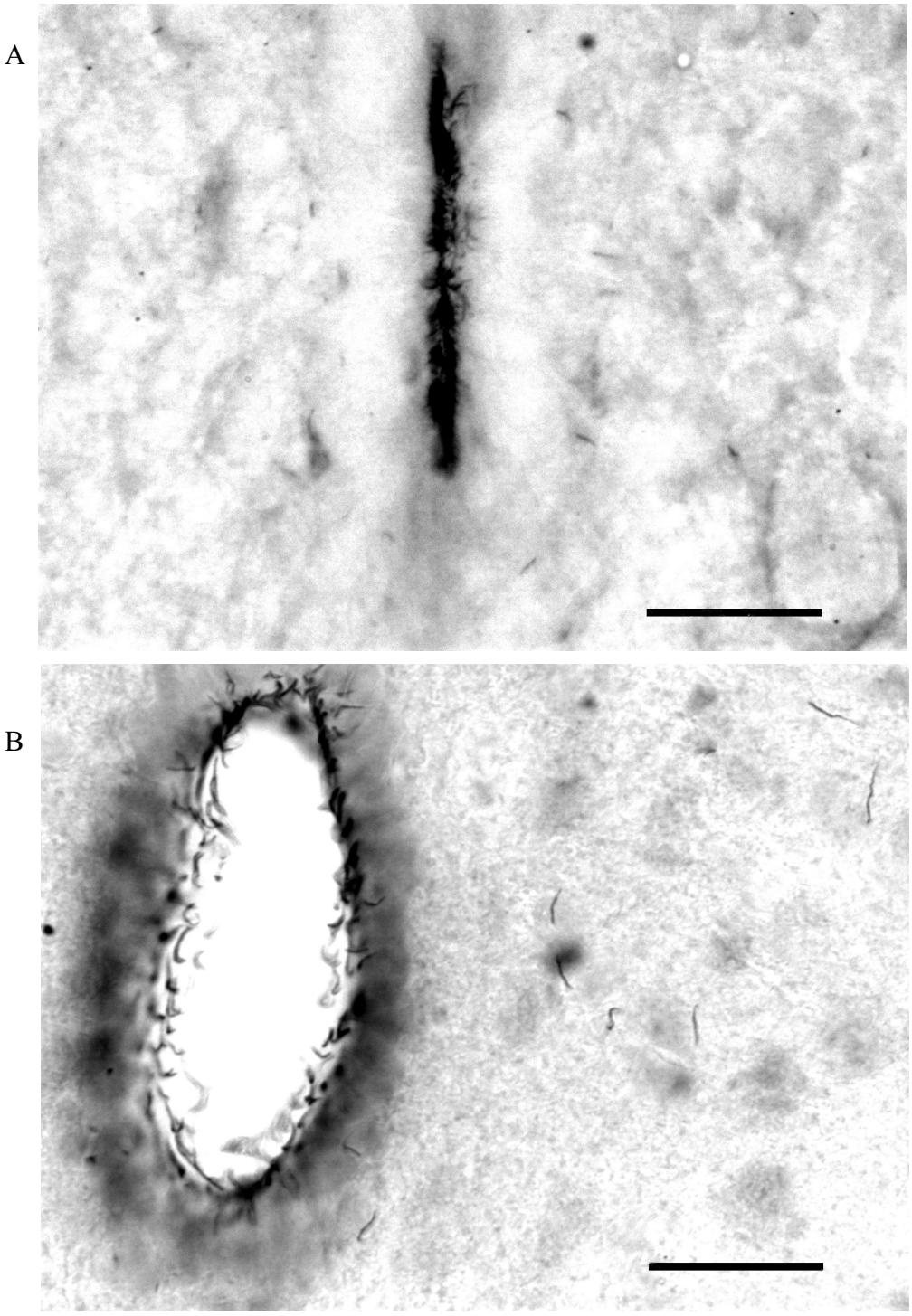

Figure 9. Ependymal and neuronal cilia of the spinal cord and central canal. Perikarya counterstained with thionin. *A,* P3 spinal tissue. *B*, Adult spinal tissue, lumbar. Scale bar = 25 μm.

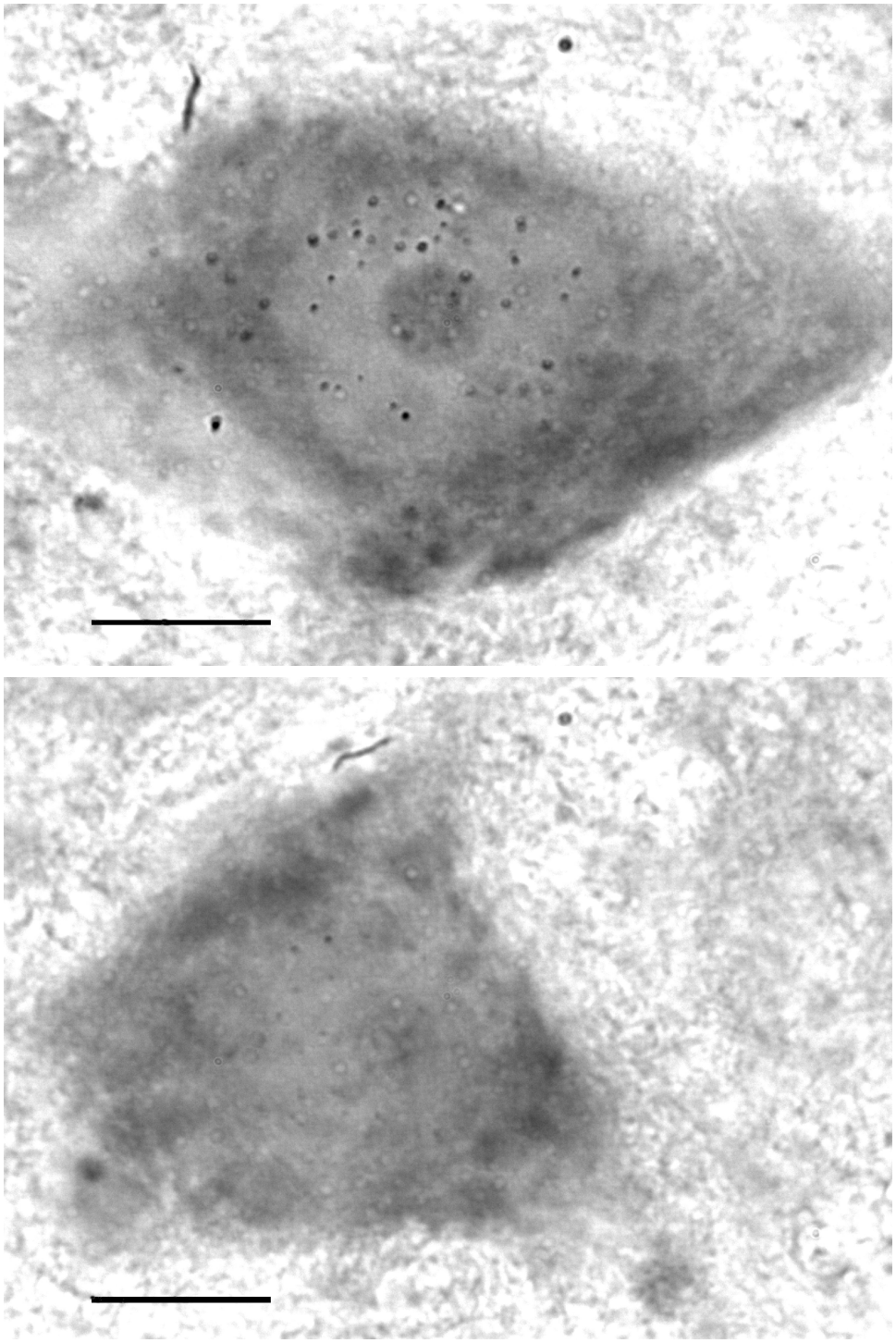

Figure 10. Neuronal cilia on motor neurons from the ventral horn of cervical spinal tissue. Perikarya counterstained with thionin. Scale bar = 10 μm.

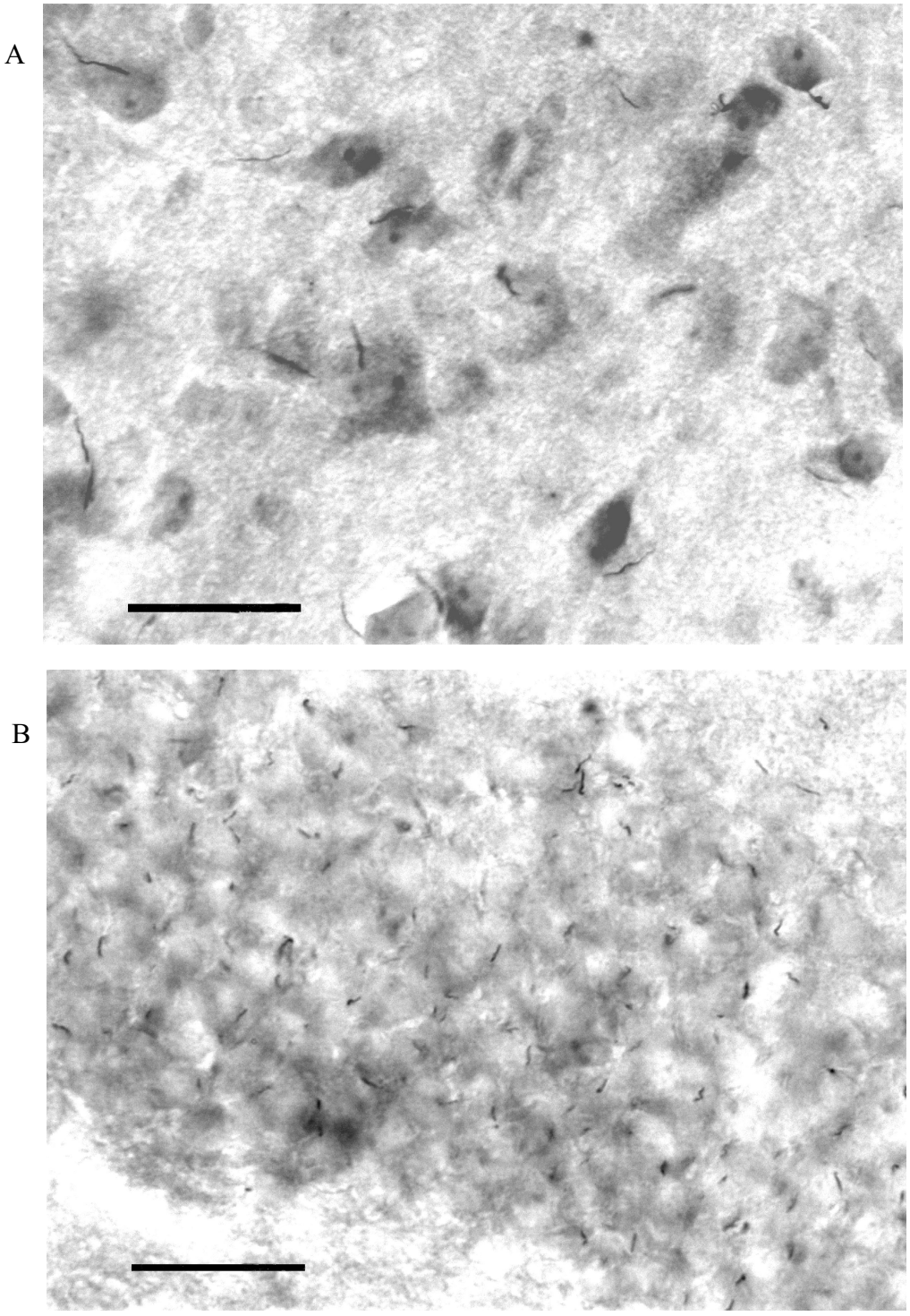

Figure 11. Neuronal cilia are expressed in a 1:1 relationship to somata, and are most often visible on the majority of somata in an area. Perikarya counterstained with thionin. *A*, Periaqueductal grey matter. *B*, Granule layer of the dentate gyrus. Scale bar = 25 μm.

DISCUSSION

Immunostaining of Neuronal Cilia

Immunohistochemical analysis of rat, mouse, and monkey tissue using an anti-$G_{\alpha 11}$, anti-$G_{\alpha q}$, and a combined anti-$G_{\alpha q/11}$ antibody revealed that neuronal (and ependymal) cilia were labeled by only the anti-$G_{\alpha 11}$ antibody, only within the CNS of the rat, and only at or after postnatal day 0. To explain the presence of $G_{\alpha 11}$-IR neuronal cilia in rat tissue but absence in mouse and monkey tissue, the following possibilities exist: (1) mice and monkeys do not possess neuronal cilia, which seems an improbable suggestion given that certain secretory cells in the pars distalis of the mouse hypophysis have been found to bear primary cilia (Barnes, 1961); (2) mice and monkeys possess neuronal cilia but these cilia do not contain $G_{\alpha 11}$ subunits; or (3) mice and monkeys possess neuronal cilia with $G_{\alpha 11}$ subunits but the subunits' region of epitope mapping is inaccessible to the antibody within these species. A complicating factor in these interpretations is the specificity of the anti-$G_{\alpha 11}$ antibody. If the anti-$G_{\alpha 11}$ antibody was indeed binding to a $G_{\alpha 11}$ subunit, it would be expected that the anti-$G_{\alpha q/11}$ antibody would also provide immunoreactivity, as both antibodies are designed to bind the same antigen. However, the anti-$G_{\alpha q/11}$ antibody did not label neuronal cilia. Thus, it could be proposed that either rats possess neuronal cilia with a $G_{\alpha 11}$ subunit which has an epitope domain accessible to the anti-$G_{\alpha 11}$ antibody but another domain inaccessible to the anti-$G_{\alpha q/11}$ antibody, or that

the anti-$G_{\alpha 11}$ antibody is binding to some unidentified component of the cilia such that no safe conclusions can yet be accurately drawn about the existence of G protein subunits in neuronal cilia.

Immunolocalization of Neuronal Cilia in the Adult Rat CNS

$G_{\alpha 11}$-IR neuronal cilia were observed in every examined region of the rat CNS that contained neuronal somata. Furthermore, the vast majority of CNS regions had a high percentage of ciliated neurons, such that most somata within these regions were found to possess a $G_{\alpha 11}$-IR cilium. In contrast, a few regions had a low percentage of ciliated neurons. An explanation for such a difference is not immediately apparent based solely upon a comparison of their anatomical locations. However, several of these regions with a low percentage of ciliated neurons are composed of a variety of cell types, including the medial geniculate nucleus, the olfactory bulb, and the cerebellar cortex, so the possibility exists that in these regions one or more cell types was expressing $G_{\alpha 11}$-IR cilia, while one or more cell types was not. For example, within the cerebellar cortex, both the outermost molecular layer and innermost granule cell layer are made up of two different cell types; basket and stellate cells within the molecular layer, and granule and Golgi cells within the granule layer (Afifi, 1998). Thus, in each layer it is conceivable that only one of the two cell types was expressing $G_{\alpha 11}$-IR cilia. However, this cannot be the only explanation for regions with a low percentage of ciliated neurons, as the Purkinje cell layer of the cerebellar cortex has only one cell type, Purkinje cells, and also exhibited a low percentage of ciliated neurons. Furthermore, there is cellular

heterogeneity in numerous other regions that exhibited a high percentage of ciliated neurons, such as in the different layers of the cortex. As in these regions the vast majority of somata were found to possess a $G_{\alpha 11}$-IR cilium, then multiple cell types must be expressing $G_{\alpha 11}$-IR cilia simultaneously.

Development of $G_{\alpha 11}$-IR Neuronal Cilia

In spinal cord tissue, $G_{\alpha 11}$-IR neuronal cilia were detected on a low percentage of somata at P0. By P3, they occurred on a percentage of somata comparable to that in adult tissue. The same was true for $G_{\alpha 11}$-IR ependymal cilia around the central canal, except they appeared at P0 on a higher percentage of ependymal cells than did $G_{\alpha 11}$-IR neuronal cilia on neurons. This pattern may reflect the development of cilia, such that ependymal cells begin expressing cilia before neurons. Alternatively, it may reflect the development of the antigen responsible for the cilia's immunolocalization, such that ependymal cells begin producing the antigen before neurons. This latter explanation may reflect an earlier physiological need for functional ependymal cilia as compared to neuronal cilia, assuming the antigen in question is one that is required for functionality, as would be a G protein subunit for signal transduction. In either case, it seems that ependymal cilia can be labeled using the anti-$G_{\alpha 11}$ antibody prior to neuronal cilia. As such, and due to the high percentage of ependymal cells expressing $G_{\alpha 11}$-IR cilia at P0, it would not be surprising to find $G_{\alpha 11}$-IR ependymal cilia in the spinal cord prior to P0, but after E18, though on fewer ependymal cells as compared to P0. As at P0 there are only a few detectable neurons expressing $G_{\alpha 11}$-IR cilia, then P0 may represent the time at which

$G_{\alpha 11}$-IR neuronal cilia are indeed first detectable using the anti-$G_{\alpha 11}$ antibody in the spinal cord, and thus $G_{\alpha 11}$-IR neuronal cilia might not be found prior to P0 as might $G_{\alpha 11}$-IR ependymal cilia.

In hypothalamic tissue, $G_{\alpha 11}$-IR neuronal cilia were not present until P3, and occurred on a lower percentage of somata than that seen in adult tissue. $G_{\alpha 11}$-IR ependymal cilia around the third ventricle, however, were visible at P0, and by P3 occurred on a percentage of ependymal cells comparable to adult levels. This situation may be interpreted as being analogous to that in the spinal cord, in which ependymal cilia can be immunolocalized prior to neuronal cilia. The reason for the absence of $G_{\alpha 11}$-IR neuronal cilia at P0 may reflect the temporal caudal-to-rostral development of the nervous system, such that at P0, the spinal cord tissue is at a more developed state (contains $G_{\alpha 11}$-IR neuronal cilia) than hypothalamic tissue (lacks $G_{\alpha 11}$-IR neuronal cilia).

Measurements of Cilia Lengths and Somata Areas in the Adult Rat CNS

$G_{\alpha 11}$-IR neuronal cilia displayed a range in mean length from 2.1 μm to 9.4 μm. Measurements of individual cilium ranged from 1.4 μm to 12.3 μm. A previous study reported measurements of individual neuronal cilium in the rat CNS ranging from 3-8 μm (Handel et al., 1999). In comparison, ependymal and respiratory cilia in the rat have been measured to have a mean length ± SD of, respectively, 8.1 ± 0.2 μm and 5.6 ± 0.5 μm (O'Callaghan et al., 1999).

In the present study, there was not an overall statistically significant correlation between cilium length and soma area, such that across CNS regions an increase in

somata areas did not predict a lengthening of $G_{\alpha 11}$-IR neuronal cilia (Figure 1). Likewise, there was not a statistically significant correlation between cilium length and soma area across the different layers of the frontal cortex (Figure 3). Measurements taken from regions with a low percentage of ciliated neurons and from different laminae of the lumbar spinal region further demonstrated a varying range of cilia lengths on somata of varying sizes (Figures 5 and 6).

There was a statistically significant negative correlation between the mean cilium length of a CNS region and the distance of that region to the nearest cavity containing cerebrospinal fluid. Thus, those regions closest to a CSF-containing cavity tended to be those with the longest cilia. This correlation is demonstrated in Figure 2. Indeed, the nine regions measured closest to a cavity included those regions with the six longest cilia measurements (above 5 μm). Figure 2 further suggests that this negative correlation was valid only within an approximate 2 mm distance to the nearest cavity. Those regions within this distance retained a statistically significant negative correlation, while those beyond this distance did not. Furthermore, those regions beyond this distance had mean cilia lengths that were shorter than the overall measured mean of 4.2 μm, with the sole exception of the subiculum. There was also a statistically significant negative correlation between the distance of a CNS region to the nearest CSF-containing cavity and that region's ratio of cilium length:soma area. Regions near CSF-containing cavities had a larger ratio of cilium length:soma area. Therefore, due to this larger ratio, the longer cilia in these regions near CSF-containing cavities were not simply the product of larger somata.

The discovery that those CNS regions in close proximity to CSF-containing cavities are those with the longest cilia is perhaps compatible with the proposal that neuronal cilia are not vestigial remnants but rather functional cellular organelles. Assuming neuronal cilia are functioning in a role similar to that of chemosensors, it would be logical to suppose that the length of the cilia would indeed be critical in determining their capability to function; longer cilia would be better suited to provide an accurate sampling of the surrounding extracellular environment. Those cilia of a shorter length might function less effectively or not at all. Thus, it could be hypothesized that the neuronal cilia in those regions near CSF-containing cavities are indeed functional and are serving as chemosensors, designed to report on the presence or absence of substances as they move out from the cerebrospinal fluid and into the surrounding interstitial fluid. This hypothesis is in accordance with current known properties of the CSF. For instance, CSF is partly responsible for maintaining the consistency of the ionic composition of the interstitial fluid and for providing nourishment for the brain, and thus there is free communication between the extracellular space of the brain and CSF-containing cavities (Marieb, 1995; Kandel et al., 2000; Bruni, 2001). Furthermore, the CSF is believed to be a transport system for the CNS, and as such contains numerous biologically active substances including releasing factors, hormones, neurotransmitters, and metabolites (Spector, 1956; Marieb, 1995; Kandel et al., 2000; Bruni, 2001).

REFERENCES

Afifi A, Bergman R (1998) Functional neuroanatomy. McGraw-Hill: New York.

Allen RA (1965) Isolated cilia in inner retinal neurons and in retinal pigment epithelium. J Ultrastruct Res 12:714-730.

Barnes BG (1961) Ciliated secretory cells in the pars distalis of the mouse hypophysis. J Ultrastruct Res 5:453-467.

Bayer VE, Pickel VM (1990) Ultrastructural localization of tyrosine hydroxylase in the rat ventral tegmental area: relationship between immunolabeling density and neuronal associations. J Neurosci 10:2996-3013.

Brailov I, Bancila M, Brisorgueil MJ, Miquel MC, Hamon M, Verge D (2000) Localization of 5-HT_6 receptors at the plasma membrane of neuronal cilia in the rat brain. Brain Res 872:271-275.

Bruni JE (2001) Cerebral ventricular system and cerebrospinal fluid. Online article: www.umanitoba.ca/faculties/medicine/anatomy/jcvindex.htm

Chalfie M, Thomson JN (1982) Structural and functional diversity in the neuronal microtubules of Caenorhabditis elegans. J Cell Biol 93:15-23.

Dahl HA (1963) Fine structure of cilia in rat cerebral cortex. Z Zellforsch Mikrosk Anat 60:369-386.

Dellacorte C, Restrepo D, Menco B, Andreini I, Kalinoski DL (1996) $G_{\alpha q}/G_{\alpha 11}$:

Immunolocalization in the olfactory epithelium of the rat (Rattus rattus) and the channel catfish (Ictalurus punctatus). Neuroscience 74:261-273.

Duncan D, Williams V, Morales R (1963) Centrioles and cilia-like structures in spinal gray matter. Texas Rep Biol Med 21:185-187.

Fuchs JL, Vu H, Israel B, Schwark HD (2000) $G_{\alpha q}$ and $G_{\alpha 11}$ immunoreactivity in rodent spinal cord. Society for Neuroscience Abstracts 26:637.

Handel M, Schulz S, Stanarius A, Schreff M, Erdtmann-Vourliotis M, Schmidt H, Wolf G, Hollt V (1999) Selective targeting of somatostatin receptor 3 to neuronal cilia. Neuroscience 89:909-926.

Kandel E, Schwartz J, Jessell T (2000) Principles of neural science: fourth edition, pp 1295-1299. McGraw-Hill Company: New York.

Karlsson U (1966) Three-dimensional studies of neurons in the lateral geniculate nucleus of the rat. J Ultrastruct Res 16:482-504.

Marieb E (1995) Human anatomy and physiology: third edition, pp 404-405. The Benjamin/Cummings Publishing Company, Inc: Redwood City, CA.

O'Callaghan C, Sikand K, Rutman A (1999) Respiratory and brain ependymal ciliary function. Pediatr Res 46:704-707.

Paxinos G, Watson C (1986) The rat brain in stereotaxic coordinates. Academic Press: San Diego.

Peters A, Palay SL, Webster H (1976) The fine structure of the nervous system: the neurons and supporting cells, pp 42-43, 90-117, 264-279. W. B. Saunders Company: Philadelphia.

Schandar M, Laugwits KL, Boekhoff I, Kroner C, Gudermann T, Schultz G, Breer H (1998) Odorants selectively activate distinct G protein subtypes in olfactory cilia. J Biol Chem 273:16669-16677.

Schwark HD, Fuchs JL (2000) Differential distribution of $G_{\alpha q}$ and $G_{\alpha 11}$ in the rat spinal cord. FASEB Journal 14:A784.

Shinohara H, Asano T, Kato K, Kameshima T, Semba R (1998) Localization of a G protein G_{i2} in the cilia of rat ependyma, oviduct and trachea. Euro J Neurosci 10:699-707.

Spector W (1956) Handbook of biological data, p 57. W. B. Saunders Company: Philadelphia.

Sotelo C, Palay SL (1968) The fine structure of the lateral vestibular nucleus in the rat. J Cell Biol 36:151-179.

Vigh-Teichmann I, Vigh B, Aros B (1980) Ciliated perikarya, "peptidergic" synapses and supraependymal structures in the guinea pig hypothalamus. Acta Biol 31:373-394.

Wheatley, DN (1995) Primary cilia in normal and pathological tissues. Pathobiol 63:222-238.

Wolfram G, Nitsch C (1992) High frequency of ciliated neuropeptide Y-immunoreactive neurons in rat striatum. Cell Tiss Res 267:199-202.